Arabian Journal of Geosciences (2018) 11: 421
https://doi.org/10.1007/s12517-018-3774-1

ARABGU2016

# The active Kalabsha Fault Zone in Southern Egypt: detecting faulting activity using field-structural data and EMR-technique, and implications for seismic hazard assessment

Z. Hamimi[1] · W. Hagag[1] · R. Osman[1] · M. El-Bialy[2] · I. Abu El-Nadr[3] · M. Fadel[3]

Received: 29 August 2017 / Accepted: 23 July 2018 / Published online: 2 August 2018


**Abstract**
Since November 14, 1981 earthquake (ML 5.6), about 60 km southwest of Aswan High Dam, the seismic hazard raised and the Aswan Local Seismic Network (ALSN) has recorded and precisely monitored the seismic activity in the vicinity of the High Dam. The major source of seismic activity in this region is the active Kalabsha Fault Zone (KFZ). The focal mechanism solutions indicate that two nodal planes strike E to ENE, with subordinate right-lateral strike-slip component and N to NNW, with left-lateral movement. The directions of tectonic extension (T) and compression (P) are NNE-SSW and NNW-SSE, respectively. Structural investigations and application of the Electromagnetic Radiation (EMR) technique reveal ongoing activity on the KFZ. Kinematic evolution of the KFZ implies faulting events with a strong movement intervened with periods of severe crushing, grinding, and even pulverization. Such tectonic processes have resulted in fault-breccia and fault-gouge. Results obtained from the present study indicate that the KFZ is not a single transcurrent wrench fault with dextral sense of movement but, instead, it represents a major dextral transtensional shear or fault zone deforming southern Egypt and plays a significant role in the structural shaping of the area to the west of Nasser Lake. Furthermore, the activity on the KFZ is most probably controlling the seismic cycle in the area. Topographic expression of KFZ is evidently realized at Sinn El-Kaddab scarp, as well as at Gebel Marawa. Frequent surface rupturing and newly recorded strong seismic activity advocate faulting reactivation supported by the EMR data, which suggest an active fault system oriented ENE-WSW and NNW-SSE affecting the KFZ, with a maximum horizontal stress (σ1) perturbing between ENE and NNW directions.

**Keywords** Kalabsha Fault Zone · Seismotectonic activity · EMR · Focal plane mechanisms

## Introduction

The Kalabsha Fault Zone (KFZ) is located to the southwest of Aswan (about 60 km to the south of the Aswan High Dam), in the south Western Desert of Egypt. Seismotectonically, the Kalabsha area, where the Kalabsha Fault extends to the east until reach the Nasser Lake, is known as KFZ. It is located between latitudes 23°23′ to 23°59′ N and longitudes 32° 00″ to 32°59′ E (Fig. 1). The area came into attention after the occurrence of the unexpected earthquake in November 14, 1981 with a local magnitude of ML = 5.6. On a regional scale, the importance of the Aswan region came from the existence of the Aswan High Dam and Nasser Lake, where their safety against all kinds of hazards, particularly earthquakes, is critical. The Kalabsha area and its environs were the subject matter of several geological and geomorphological studies (e.g., El-Shazly 1954; Attia 1955; Issawi 1969, 1973, 1978, 1982, 1987; Woodward-Clyde Consultants 1985). The seismicity of Aswan area was regionally treated in many works (e.g., Kebeasy et al. 1981; Maamoun et al. 1984; Woodward-Clyde Consultants 1985; Ambraseys et al. 1994; Awad and Mizoue 1995; Abu Elenean 2007; Haggag et al. 2008), whereas detailed fault plane solutions of earthquakes were achieved (e.g., Kebeasy et al. 1987; Kebeasy and Tealab 1997; Hassib 1997; Abu Elenean 1997; Tealeb 1999; Fat-Helbary and Tealeb 2000;

This article is part of the Topical Collection on *Current Advances in Geology of North Africa*

✉ W. Hagag
waelhagag78@yahoo.com

[1] Geology Department, Faculty of Science, Benha University, Benha 13518, Egypt

[2] Geology Department, Faculty of Science, Port Said University, Port Said 42522, Egypt

[3] Seismology Department, National Research Institute of Astronomy and Geophysics, Helwan, Egypt

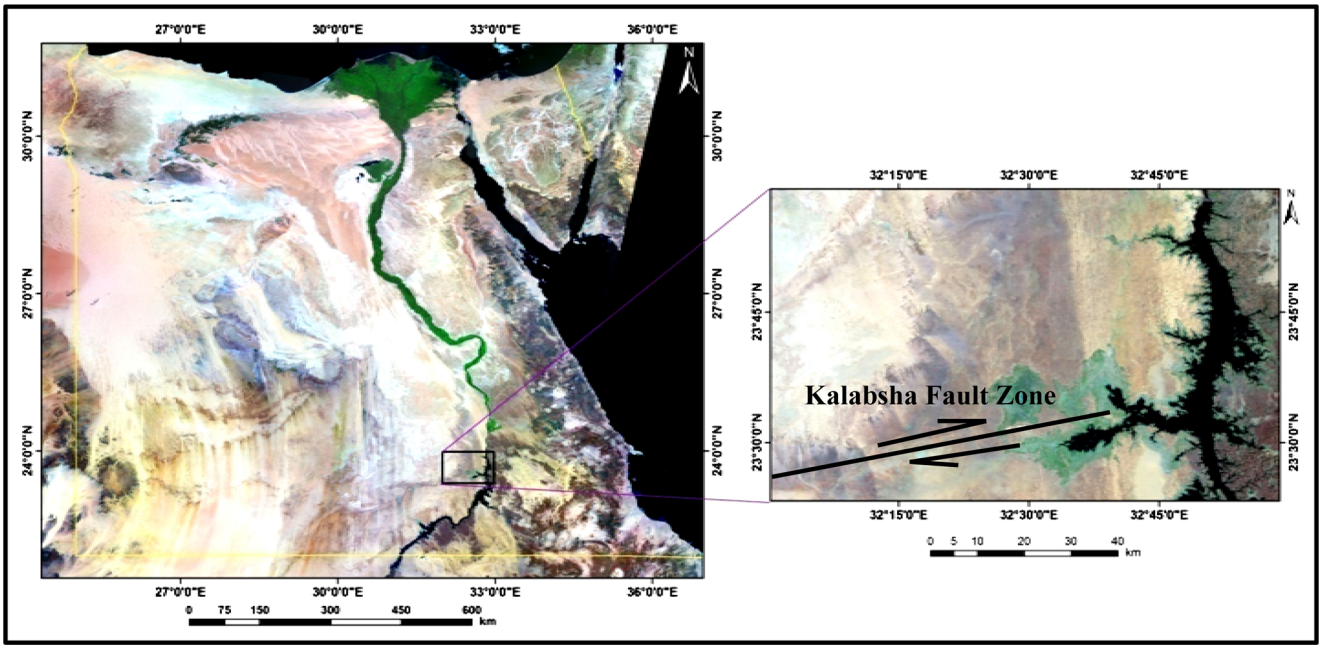


**Fig. 1** Location map of the study area

Badawy 2001; Hussein et al. 2013; Hosny et al. 2014; Abdelazim et al. 2016). Limited work has been done on the subsurface tectonic structures and crustal deformation (e.g., Mahmoud 1994; Taha 1997; El-Hady et al. 2004; Khalil et al. 2004; Mekkawi et al. 2008); however, the considerable investigations of the geological structures on surface exposures were displayed (e.g., El Etr et al. 1982; Woodward-Clyde Consultants 1985; Stern and Abdelsalam 1996; Guiraud and Bosworth 1999; Thurmond et al. 2000; Abdeen et al. 2000; Guiraud et al. 2001; Thurmond 2002; Thurmond et al. 2004). The main objective of the present work is to explore the main causes of the seismotectonic activity along the KFZ in relation to the major structural and tectonic trends dissecting the Aswan region. For better understanding of the mode of seismotectonics in, and around, Nasser Lake (the eastern extension of the KFZ), the earthquakes epicentral distributions and the nature of their focal mechanism solutions have been studied. In addition, for analysis of the ongoing activity and the present day direction of the maximum horizontal stress on the KFZ, the EMR-technique was applied as a complementary method. Detailed field-structural work has been achieved to investigate and define the different effective structural and tectonic trends that control the seismotectonic activity along the study area.

## Lithostratigraphy

The sedimentary succession exposed in the study area is lithostratigraphically subdivided into several rock units ranging in age from Precambrian to Quaternary (Fig. 2). Herein, we followed the work of Issawi and Osman (1993) in the classification of and description of the exposed rock units in the study area.

### The Neoproterozoic basement

The basement rocks form relatively small domal inliers composed of gneissose granite (Fig. 3a) that nonconformably underlies a series of sedimentary units of Late Cretaceous-Early Eocene age. These rocks are exposed at sparse occurrences west of the Nile River between the Kalabsha Fault in the south and Aswan City to the north (Issawi 1978; Woodward-Clyde Consultants 1985), besides those outcropping to the east of the Nasser Lake. It is obvious that these basement rocks were exposed due to a tectonic uplift along the major E-W oriented faults (Guiraud and Bosworth 1997).

### The Paleozoic sediments

#### The Wadi Malik Formation (Devonian)

The Devonian section at Gebel Um Shaghir (25 km to the south of the main scarp of the Kalabsha Fault) can be correlated with that of Issawi and Jux (1982) described in Aswan area. Depending on the trace fossils recorded in the upper part, the section is divided into two parts, lower and upper. The section is made up of pale red, medium hard, and fine grained sandstone at the base grading upward into hard, brownish to reddish yellow, and fine to coarse grained sandstone beds. Conglomerate beds are present and composed mainly of quartz pebbles. Clay intercalations are common in the middle part of the section, while Kaolinized beds are rare. The

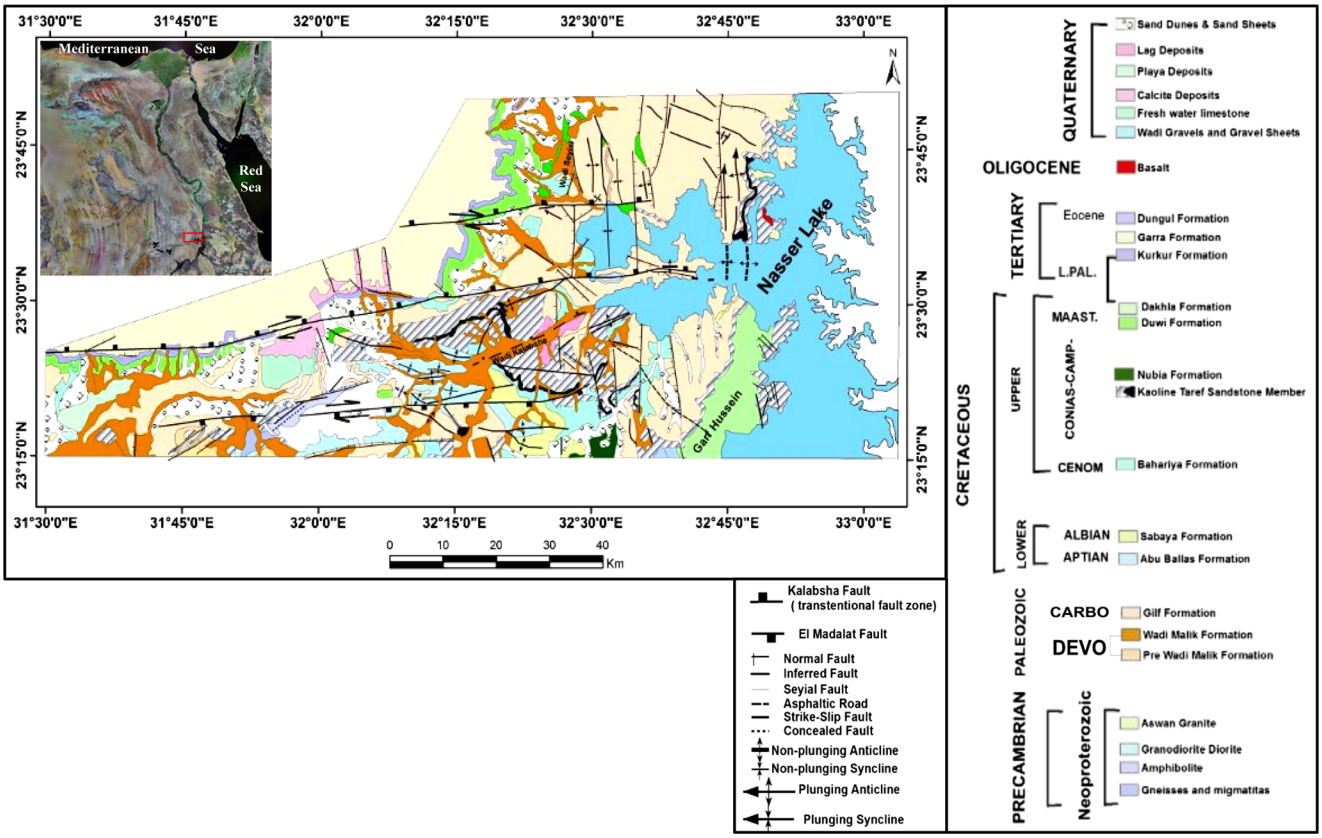


**Fig. 2** Geological map of the study area (modified after Issawi and Osman 1993)

formation can be only recognized from the overlying Gilf Formation by the occurrence of a very hard, 1.0-m-thick conglomeratic bed at their mutual contact.

### The Gilf Formation (Carboniferous)

The Gilf Formation is exposed at the southwest of Gebel Kalabsha. South of the Kalabsha kaolin quarries, it covers the core of the anticlines and faulted ridges. Most of the hills and hummocks overlying Precambrian rocks consist of Gilf Formation. The Gilf Formation consists of a sequence of tabular cross bedded sandstone interbedded with thick and structurless sandstone beds. In places, the section near the Precambrian basement contact is rich in very coarse grained kaolinitic and conglomeratic patches. Also, the sandstone is well-sorted and fine grained, but in other places is composed of fine to coarse sandstone beds rich in quartz pebbles. Kaolinized sandstone beds are common intercalations within the formation. Conglomeratic layers are frequently encountered between the sandstone beds especially near the basement contact. At El Maddallat hills (Fig. 3b), the Gilf Formation is well exposed and composed of very coarse gritty sandstone which becomes finer upward. The Gilf sandstone is very poor in fossils except silicified woods found to the south of Gebel Barq El-Sahab buried under the alluvial deposits. According to the composition and stratigraphic position, the Carboniferous age was assigned to the formation (Issawi and Jux 1982).

## Mesozoic Rocks

### The Abu Ballas Formation (Aptian)

The formation is exposed at the southern part of the area, where it covers most of the Nubian plain around Gebel Barq El-Sahab. The Abu Ballas Formation is composed of hard, very fine, and well-sorted sandstone. Sandy clays and marls are the main intercalations (Fig. 3c). Due to the presence of ferruginous beds, the color of Abu Ballas Formation is dark in contrast to the underlying and overlying units. The contacts with the overlying and underlying rock units are characterized by unconformable relationships. Jointing or fracturing in some outcrops is observed in Abu Ballas Formation.

### The El Sabaya Formation (Albian)

El Sabaya Formation crops out at the southern part of the area forming most of the major residual hills. It consists of sandstone beds rich in kaolin bands and paleosols, as well as minor clay. The sandstone beds are hard to friable, thick bedded, and light in color with grain size that ranges from fine to coarse.

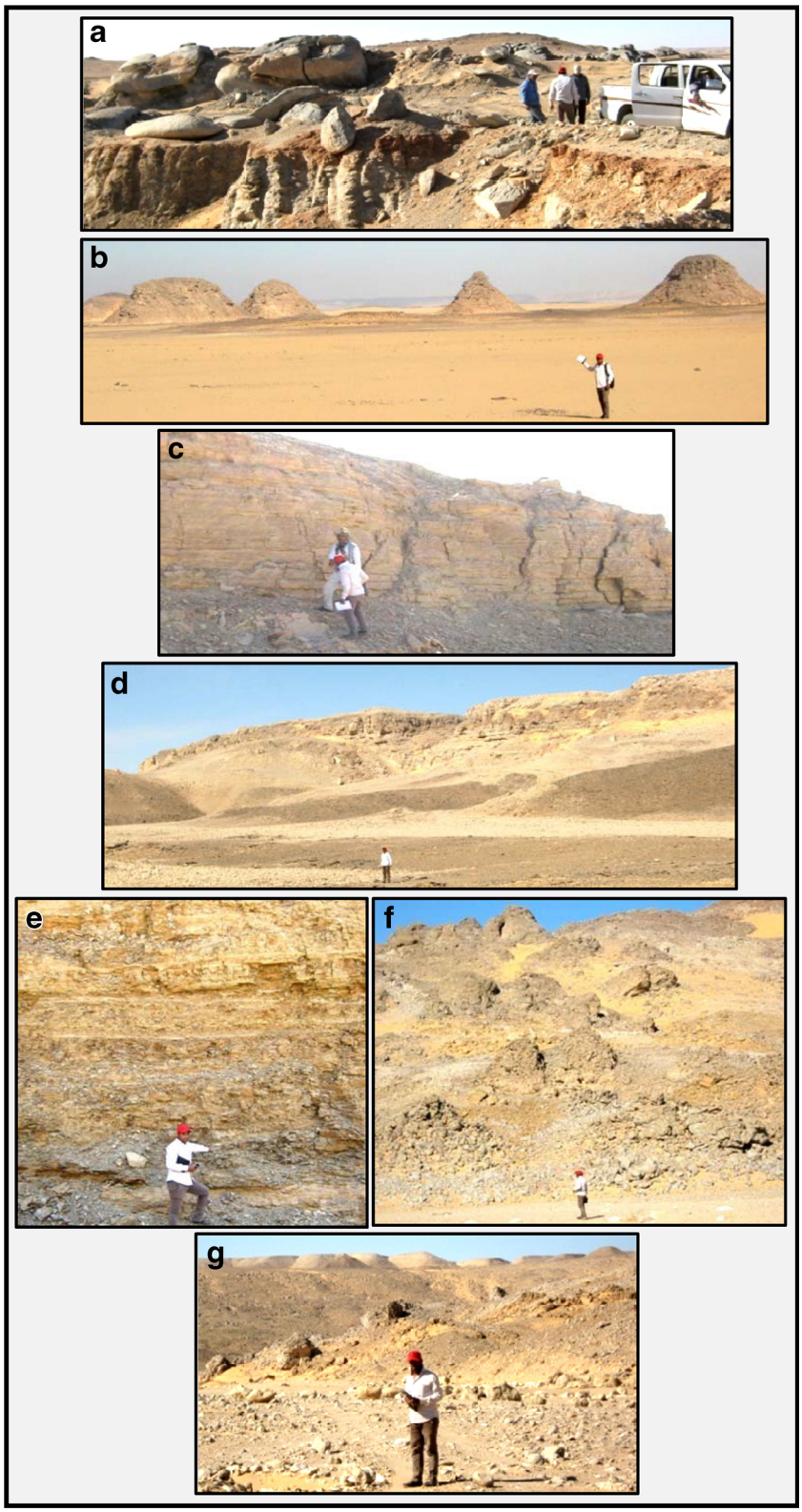


**Fig. 3** Field photographs for some exposed lithostratigraphic units: **a** domal pulses of gneissose granite to the south of El Madallat area, **b** Gilf Formation in El Madallat hills, **c** Abu Ballas Formation around Gebel Barq-El Sahab, **d** Nubia Formation abutting southern scarp of Gebel Kalabsha, **e** Dakhla Formation at foot slopes of Sin El-Kaddab Plateau, **f** Kurkur Formation forming the face-scarp of Sinn El-Kaddab Plateau, and **g** Garra Formation capping Kurkur Formation at the extension of Gebel Kalabsha Scarp

Sandstone is generally ill-sorted to moderately sorted. Kaolintic sandstone beds are common within the formation, where these beds range in thickness from few centimeters to 1.70 m including quartz pebbles and ferruginous intercalations. Paleosol bands are frequent at Wadi Kalabsha and mainly composed of sandy siltstone with hard ferruginous roots. The contact of the formation with the overlying and underlying rocks is unconformable. Plant remains in El

Sabaya Formation along with its stratigraphic position relegate the Early Cretaceous age to this formation.

### The Bahariya Formation (Albian-Cenomanian)

The Baharia Formation covers most of the hillocks west of the Nasser Lake. It is composed of alternating varicolored sandstone, sandy clay, and siltstone. The sandstone beds are hard, fine-grained, grayish white, generally well sorted, and partly Kaolinized. The clayey-sandstone interbeds are dark, partly ferruginous, and assuming parallel stratification with rippled bedding surfaces. The most characteristic feature is the hard oolitic iron bands, which are in most cases cap the Baharia Formation. The thickness of the formation highly depends on the paleorelief. Generally, some plant fossils are present at the bedding planes of the ferruginous bands, especially at the middle part. The age of the formation is determined based on the good preserved fossils such as *Neolobites vebrayeanus*, *Exogyra flabellate*, and *Exogyra mermeti*, which assigned a Lower Cenomanian age to the formation.

### The Nubia Formation

In the study area, the Nubia Formation is the main rock unit that covers the Nubian Plain. It covers most of the Wadi Kalabsha at its southern part and also crops out at the foot slopes of the scarp between Gebel Kalabsha and Dungul Oasis. In this stretch, the formation forms extensive plains, as well as high scarps, isolated hills, and hummocks (Fig. 3d). This formation is classified into two members: Taref Sandstone Member at the base and Qusier Clastic Member at top.

**Taref Sandstone Member (Coniacian-Santonian)** The Taref Sandstone Member is composed of sandstone, grits, conglomerates, and paleosols. Sandstones form most of the succession and are varicolored, ill-sorted, and coarse to fine grained. Conglomerate beds are frequent at the lower part of the member and on top of the Precambrian rocks, where boulders of coarse grained sandstone are found. Paleosol beds are most frequent in the member and these beds are violet to bluish gray including hard brown ferruginous sandstone with root casts. Both the upper and lower boundaries of this member show unconformable relationships with the other rock units. Though the Member is poor in fossil content, the stratigraphic position that overlie the Bahariya Formation of Cenominian age and underlie the Quseir Clastic Member rich in *Inceramous regular* substantiates the Coniacian-Santonian age.

**Quseir Clastic Member (Campanian-Maasterichtian)** The Quseir Clastic Member crops out at the foot slopes of Sinn El Kaddab scarp and extends eastward to the western Nile bank. It also forms the foot slopes of Gebel Kalabsha–Bir Dungul stretch. The basal part of the member is mainly composed of shales with few sandstone bands. Paleosol beds are more frequent at the lowermost part, while Oolitic iron bands occur among the clastic beds and in places are connected with conglomeratic lenses. At Barq El Sahab-Um Shaghir stretch, the section being composed of laminated kaolinized clayey sandstone which includes light orange oolitic iron bands and very fine hard sandstone beds. The middle part of the Quseir Clastic Member is composed of cross bedded sandstone alternating with massive thick banded sandstones. The upper part of the Quseir Clastic Member is highly variable in lithology, where it changes from shale to sandstone. The sequence started at the base with hard marl and upward fine laminated, rippled sandstone beds build up the rest of the section. In most outcrops, the Duwi Formation is missing and the Dakhla Shales unconformably overlie the Quseir Clastic Member. Due to the presence of *Inoceramous regularis* and other floral contents, the Quseir Clastic Member can be regarded as of Upper Senonian age.

### The Duwi Formation (Campanian-Maasterichtian)

This formation has very limited areal extent and crops out near the foot slopes of Sinn El-Kaddab plateau in the form of small mesas and buttes. North of Gebel Barq-El Sahab, the Duwi Formation crops out in the form of lenses on the top of the Quseir Clastics. The section is composed of shale at the base with few very fine, laminated sandstone intercalations. The shale is capped by hard, conglomeratic, and laminated phosphatic marl. The Duwi Formation is overlain by a thick succession of Dakhla Shale with a pronounced unconformity surface marked by a conglomeratic band. Some of the sandy shale beds show rich foraminifera content, shark teeth, and bone fragments, which indicate an Upper Cretaceous age of this unit.

### The Dakhla Formation (Maasterichtian-Danian)

In the study area, the phosphatic beds of the Duwi Formation are not well represented and the proper sandstone beds of the Nubia Formation are overlain by a shale section with carbonate interbeds, known as the Dakhla Formation (Fig. 3e). It composes the lower part of Sinn El-Kaddab scarp, as well as the lowermost part of Gebels Marawa and Barq-El Sahab. The formation is made up mainly of greenish gray shale beds interbedded with sandstone at the base and intercalated with carbonates near the top. The age of the Dakhla Formation is Maastrichtian at the base and Danian at top.

## Tertiary Rocks

### The Kurkur Formation (Danian-Landenian)

The Kurkur Formation overlies the shale beds of the Dakhla Formation with seeming conformity. The general brownish

color of this formation contrasts with the underlying greenish to grayish colors of the Dakhla beds and with the white chalky limestone beds of the overlying Garra Formation. The formation outcrops along the scarp faces of Sinn El-Kaddab plateau, between Gebel Garra in the north and Gebel Kalabsha in the south (Fig. 3f). Westward, the formation is well exposed forming most of the scarp face and also the upper slopes of Gebel Marawa as well as the basal part of Barq-El Sahab hill. The Kurkur Formation is made up of two thick carbonate beds interbedded with shale and sandstone beds, having a total thickness of 11 m at Wadi Kurkur.

#### The Garra Formation (Landenian-Ypresian)

Capping the Kurkur Formation is well recognized along Sinn El-Kaddab scarp at the escarpment of Gebel Kalabsha (Fig. 3g) and topmost part of Gebel Marawa, owing to its white or pale colors that contrast with the underlying dark colored Kurkur beds. The lower contact is also characterized by a local unconformity. The contact with the overlying Dungul Formation is marked by the appearance of Nummulites which are abundantly present at the lower beds of the Dungul Formation. The Garra Formation consists of thick limestone beds with chalk, marl, and shale intercalations. The limestone beds are hard, thick bedded, and partly cavernous. Flint bands are common in the limestone beds. The most important fossils found in the Garra limestone beds are *Lucina thebaica*, *Schizaster chargensis*, *Terbretulina chrysalis*, and *Schizorhabdus libycus*. This fossil assemblage indicates the Upper Paleocene-Lower Eocene age to the Garra Formation.

#### The Dungul Formation (Ypresian)

Huge blocks of Dungul limestone are noticed at the foot slopes of Gebel Kalabsha. These blocks fall from the Dungul scarp which once made the summit of Gebel Kalabsha before it retreated westward. Another small outcrop of the Dungul limestone is mapped west of Gebel El Digm. The Sinn El-Kaddab plateau is covered by Dungul Formation and most of its surface extends westward outside the study area. The formation is composed of white limestone with few marl intercalations. Shale and flint nodules are rare in the Dungul sequence. The Dungul beds include *Nummulites praccursor*, *Nummulites irregularis*, and *Operculina* sp. These fossils gave a Lower Eocene age to the Dungul Formation.

### The Quaternary deposits

The Quaternary deposits include several types of sediments which are related primarily to climatic fluctuations between pluvial, semiarid, and hyperarid phases. Deposits of the wet phases are represented by playas, slope wash, alluvial deposits, tufa, and calcite deposits. The arid phases resulted in, however, extensive sand sheets and dunes and lag deposits.

## Structural setting of the Kalabsha Fault Zone

### Non-tectonic structures

Since the study area has a unique stratigraphic succession that comprises both clastic and carbonate rock units, several primary sedimentary structures have been encountered and described. These structures help to determine the way-up direction of sequences and also have been used as strain markers within the KFZ. Stratification and lamination are the main sedimentary structure as many outcrops have well-defined strata and substratum laminae (Fig. 4a). Cross-stratification is a dominant sedimentary structure easily recognized within the clastic rock units covering a vast tract in the study area. The Gilf Formation is made up of a sequence of tabular cross bedded sandstone interbedded with thick and structureless sandstone beds (4b). Also, the main sedimentary structure in El Sabaya Formation is tabular cross-bedding. The thickness of sets and the azimuth of foresets, as well as the dip angles of laminae, are different from place to place reflecting several wind directions. Tabular and trough cross-stratification, convolute bedding (Fig. 4c), and linguoid ripples (Fig. 4d) are the dominant sedimentary structures of the Taref Sandstone Member. The thickness of the bed ranges from few centimeters to 1.5 m, while the thickness of the foreset laminae is less than 1 cm. The foreset beds dip 12° to 25° in N and NW direction. Graded bedding, mud cracks, and rain prints are also frequent sedimentary structures recorded within the rock succession of the studied area (Fig. 4e). The reduction spots are of great importance where they have been recognized in the ferruginous sandstones of the Nubia Formation (Fig. 4f) as a mottled spherical area of sediment that has been oxidized during digenesis (Spinks et al. 2010). A unique sedimentary structure has been recorded in the clastic sediments of the Abu Ballas Formation. This structure resembles the "liesegang structures" (Haakon Fossen, personal communication) and is most probably formed by fluids flowing along a fracture network and infiltrating through the host rock altering its composition (Fig. 4g).

### Tectonic structures

Secondary tectonic structures are mainly represented in the study area by KFZ and subsequent shear zone-related structures.

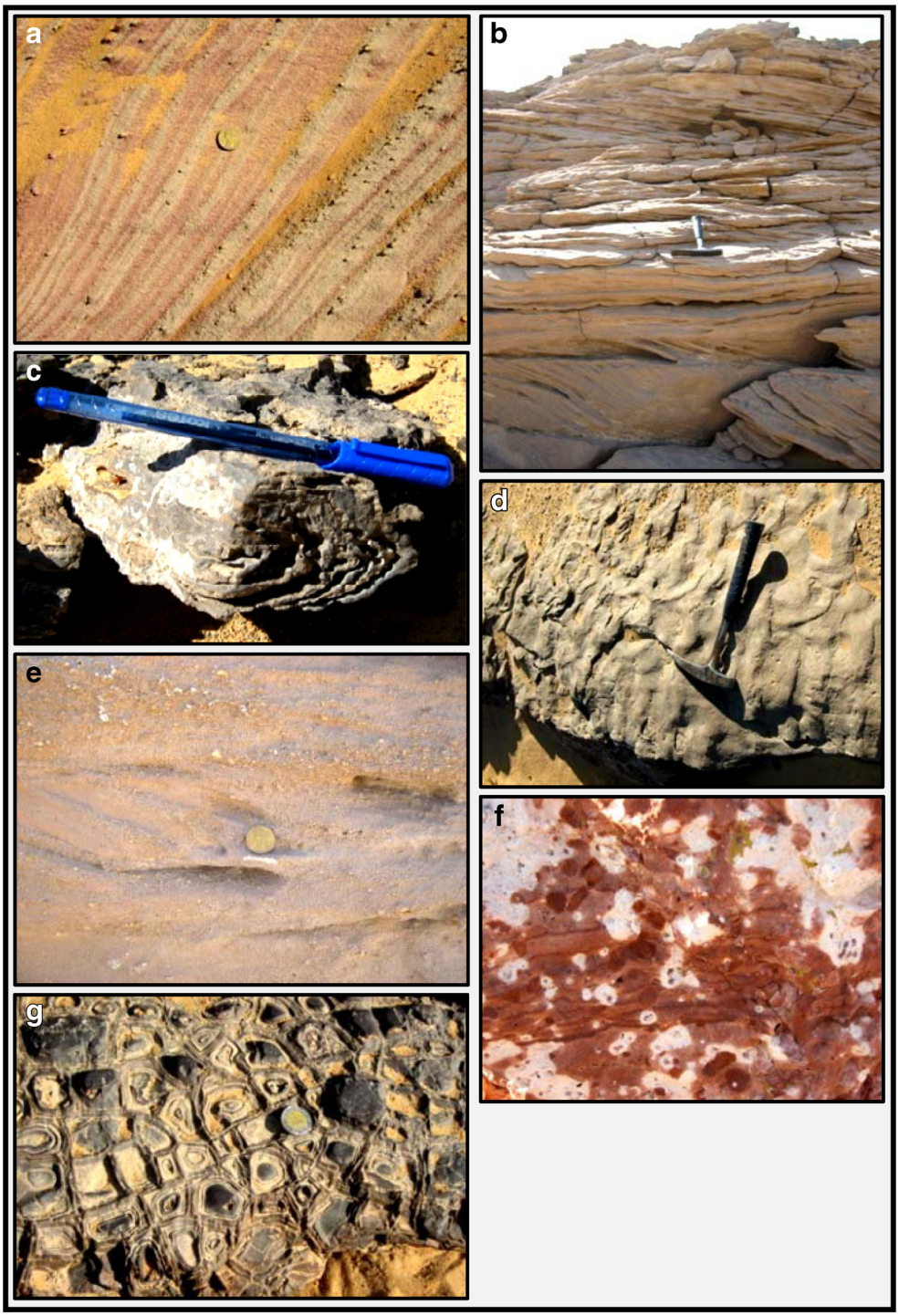


**Fig. 4** Primary sedimentary structures demonstrated in the study area: **a** laminated sandstone, **b** tabular cross-bedding, **c** convolute bedding, **d** linguoidal ripples, **e** graded bedding, **f** reduction spots ferruginous sandstones, and **g** liesegang structure

## Kalabsha Fault Zone

**Attitude and geometry** The KFZ is one of the main morphostructural discontinuities that occurred within a vast region binding southern Egypt and northern Sudan. The structural studies of Thurmond et al. (2000) and Thurmond (2002) on southern Egypt and northern Sudan suggested that the E-W trend is relatively younger (?) than the N-S trend and its faults have an average spacing of 5–10 km particularly in the Nubian Plain. The Late Cenozoic faults in southwestern Egypt have occurred in two fault trends, N-S and E-W, where the E-W faults have strike-slip movements and dissect the Nubian plain and Sinn El-Kaddab plateau. Among the kinematic mechanisms, crustal rupture or ground cracks in the

Nubia Formation explain the prevalence of E-W faults (Stern and Abdelsalam 1996; Thurmond et al. 2004), an uplift of Precambrian granite along a propagated segment of the Guinean-Nubian Lineament (Guiraud and Bosworth 1997) and E-W trending faults related to the Tethyan tectonics (Meshref 1990). The major faulting displacement is a strike-slip with a minor vertical dip-slip component produced low scarps along most of the length of the faults (Woodward-Clyde Consultants 1985). Slip-tendency studies by Woodward-Clyde Consultants (1985) reveal that the E-W striking faults had greater degree of activity and longer total displacements than the N-S trending faults. Also, the slip rates on E-W faults are about 0.03 mm/year and on N-S faults have lower slip rates, 0.01 to 0.02 mm/year. The age relationship between the E-W and N-S fault trends is a matter of debate. They were interpreted to be coeval sets with conflicting cross-cutting relationships (El Etr et al. 1982). The regional basement uplift has played a noteworthy role in the structural pattern of Kalabsha area, where it was associated with regional faulting, whereas folding was of secondary effect and folds are either associated with faulting or uplifted basement blocks (Issawi 1968). On Landsat image (see Figs. 1 and 2), the KFZ is characterized by a total length of about 300 km. The master fault is extended eastward from Gebel El-Digm to the Nasser Lake, with a continuous trace of approximately 185 km. The actual extent of the KFZ beyond the realm of the Nasser Lake in the Eastern Desert is controversial.

KFZ is a wide accommodation zone, where the extensional to transtensional localized strain can be consumed along the ENE to NE oriented extensional fractures and open cracks in a progressive evolution deforming the lower crustal levels and induce microseismic events. The entire zone cannot be represented by a single fault, but it is a major fault or shear zone, as well as it changes its geometry along different segments at its vicinity. The Kalabsha Fault changes its orientation some 5 km to the east of Gebel Marawa (Woodward-Clyde Consultants 1985). Approximately 160 km to the west of Gebel Marawa, a single clearly defined trace of the main Kalabsha fault with a fault ridge composed of Nubia Formation, overlooking the southern Nubian plain and abutting a subdued Late Cretaceous Dahkla Formation (Fig. 5a).

**Sense of shear** Identification and characterization of neotectonic events are of special interest to estimate seismic hazards attributed to a high rate of seismicity and tectonic activity. The type of faulting and the direction of displacement on a fault plane are most important features in relation to the size of earthquake. The present study indicates that the master fault of Kalabsha has a dominant strike-slip movement with minor vertical normal dip-slip component (transtensional movement). The sense of the strike-slip displacement on the KFZ is dextral. It marks the southern escarpment of the Sinn El-Kaddab Plateau. Several lines of evidence indicate that KFZ has a right-lateral sense of displacement: structural geometry of the fault traces and associated structures, focal mechanisms of associated earthquakes, and the direction of displacement of geomorphic units.

At Gebel Marawa, the geometry and timing of faulting on the KFZ imply a major faulting event with a strong movement passing into periods of crushing, grinding, and even pulverization. The net result of these tectonic processes gives either fault breccia or fault gouge. Therefore, these types of fault rocks provide tangible evidence or criteria on the kinematic processes that once operated along such major fault zone. From field-structural observations, the relatively wide open fractures filled with fault breccia and fault gouge with different colors attest heterogeneous strain along the KFZ and repeated rejuvenation on some fault segments. In addition, the presence of fault gouge sealing certain planes and its lack on others demonstrates a major fault zone rather than a single penetrative fault. Fault gouge is a common product of cataclastic deformation working in low pressure and temperature conditions. In the same context, fault breccia is a common fault rock along upper crustal levels, particularly in the top few kilometers, where the potential for dilatational strain increases makes the range of breccia formation processes more possible. At Gebel Marawa, fault brecciation has been recorded and is a clear-cut kinematic indicator (Fig. 5b). Similarly, fault breccia filling dilatational fractures at Gebel Kalabsha main scarp was also documented (Fig. 5c). Examination of the kinematic indicators to the east of Gebel Marawa revealed subhorizontal slickenlines striking ENE (080°) and dipping 30° SSE. The remarkable offsetting of the E-W oriented faults along the Kalabsha Fault Ridge by the N-S oriented faults (Fig. 5d) indicates that either the E-W faults are older or the two trends are conjugate, but the N-S trend is lately rejuvenated.

**Shear zone-related structures** As indicated above, the KFZ is not a single wrench fault but it is a fault zone that demonstrates complex structural geometry and kinematic history. Shearing along KFZ led to the formation of shear zone-related structures such as domes and basins. These structures are observed along with the E-W and N-S trending fault zones of the Western Desert of Egypt (Tewksbury et al. 2009; Hogan et al. 2013). As a result of the wrench movement along the KFZ, transpression (restraining bend) and transtension (releasing bend) deform bedrocks at certain areas and create low-relief structural basins. Domal or anticlinal structures have been demonstrated in the vicinity of Kalabsha area as isolated hills cropping out on the Nubian plain. One of such domal structures has a Precambrian diorite core and is flanked by Mesozoic clastics capped by post-Mesozoic gravels (Fig. 5e). There are two proposed kinematic mechanisms to account for the formation of domes, due


**Fig. 5** Field photographs represent some structural features discriminated along the Kalabsha Fault Zone: **a** well-defined Kalabsha Fault with a ridge made up of Nubian sandstone abutting a subdued plain of the Late Cretaceous Dahkla Formation, **b** fault breccia and fault gouge filling the well-defined E-W oriented open fractures at Gebel Marawa, **c** fault breccia filling the dilatational fractures at the main scarp of Gebel Kalabsha, **d** the N-S oriented faults remarkably offsetting the Kalabsha Fault scarp, **e** a domal structure cored with Precambrian diorite and flanked by Nubia Sandstone strata, **f** shallow synclinal basin with axial surface strikes 040° and dips 55 SE, south of El Madallat area, and **g** E-W oriented sand channels indicate an ongoing activity on the KFZ

to the emplacement and upheaving of Precambrian diorites or they are intruded post-dating domes as a consequence of exhumation and uplift related to the complex shear deformation along the KFZ. At the eastern edge of the Sinn El-Kaddab plateau and a nearby Nasser Lake, a synclinal basin was observed, where it is made up of ferruginous sandstone of the Nubia Formation and Tertiary sediments (Fig. 5f), with an axial surface strikes N40° E and dips 55° SE.

Overall, the aforementioned structures and also the shear criteria discussed above are rather evidence of a transtentional

shear zone characterized by major segments of wrench faults that show a minor component of dip-slip movement. Large open fractures follow the same E-W trend and approximately filled in places with fault breccias and gouges suggest extensional stresses accompanying wrenching regimes. Again, subhorizontal slickenside lineations recorded along some fault traces and bedding surfaces at several locations, such as the main Kalabsha Fault Scarp, to the west of Gebel Kalabsha and Gebel Marawa reveal strong successive wrenching movements. However, the occurrence of long ground channels oriented generally E-W (Fig. 5g) and filled with wind-blown sands give a good sign for the ongoing activity on the major E-W faults dissecting southern Egypt and especially deform the KFZ.

## EMR data

### General outline

The electromagnetic radiation (EMR) technique facilitates the investigation of geological structures and related stress regimes. Such technique is based on the natural electromagnetic waves emitting from brittle materials when exposed to mechanical stresses. Although it is an old phenomenon, it has been recently tested for applicability in the field of structural geology. Micro-fracturing related charge transfer is proposed to be the main geogenic source of the EMR among other possible processes. For basic principles of EMR and its application in structural geology and neotectonics, it is recommended to read the basic works of Bahat et al. (2005) and Greiling and Obermeyer (2010). Of the recent works on the EMR-Technique and Cerescope in the investigation of geological structures are those of Reuther et al. (2002), Lauterbach (2005), Lichtenberger (2005, 2006a, b), Mallik et al. (2008), Reuther and Moser (2009), Hamimi and Hagag (2017), and Hagag and Obermeyer (2017). In the present work, the EMR-technique and the Cerescope are applied for surface detection of the active fractures and identification of the maximum horizontal stress direction $\sigma_H$ along the Kalabsha Fault Zone in southern Egypt. Two major linear EMR profiles are measured using Cerescope (Fig. 6a) to define the location and, to some extent, the style of the different active faults or fault segments that have deformed the sedimentary succession exposed in the Kalabsha area. Horizontal EMR measurements are also recorded to recognize the direction of maximum intensity of EMR that is directly in relation with the orientation of the maximum horizontal stress axis ($\sigma_1$). The results of the linear and horizontal EMR data, structural-field, and seismic data analyses will be discussed in the frame of the ongoing seismotectonic activity on the Kalabsha Fault Zone.

### Methodology

In all EMR studies, measurements are taken with the Cerescope (Fig. 6b). The hardware, adjustment steps, and functionality of the Cerescope were described with details in Obermeyer (2001, 2005). The values measured by the Cerescope are stored as parameters A to E. Parameter A defines the number of peaks crossing the discrimination level, while parameter B is the number of counted bursts. Parameter C measures the average amplitude of bursts, whereas the energy and the mean frequency of bursts recorded as parameter D and parameter E, respectively (Table 1). Parameters A and D are the most useful EMR data measured for meaningful interpretation. As described by Obermeyer et al. (2001), linear EMR measurements are recorded along linear profiles. They are taken for detection of the site of active faults and stress loci. Linear profiles are usually performed in a time-triggered mode with a regular speed to produce a uniform distribution for the measured points. As a consequence, in mountainous regions and long profiles of kilometer length, the measurements can be taken with a car of regular speed to make a regular spacing between individual measurements. Meanwhile, it is possible to determine the main horizontal direction of EMR using horizontal measurements. Assuming that the EMR are generated along the tensional micro- and nano-cracks, the main radiation direction will be coincided with the preferred orientation of the cracks and therefore allows the determination of the direction of the main horizontal normal stress ($\sigma_H$). During horizontal measurements, the beam antenna is moved in a circle, with a 360° azimuth, at a horizontal plane. One measurement will be taken each 5° interval, produced 72 measurements at each location. An alternative method is to fix the antenna on an automatic mode, using a rotating device.

### EMR measurements along the Kalabsha Fault Zone

EMR measurements are recorded by the Cerescope along two linear profiles (see Fig. 6a), generally oriented N-S and running across the Kalabsha Fault Zone that strikes E-W. As the area is characterized by rugged surface and moderate to high mountainous peaks, EMR measurements are taken using a four-wheel-drive vehicle. The Cerescope device is adjusted on the highest level of gain 4 during all measurements, while the antenna of the Cerescope oriented perpendicular to the ground surface. The measurements were operated in several days during December 2015, with suitable conditions for EMR working. The time interval 10:00 am to 03:00 pm are chosen to avoid the artificial signals from the VLF transmitters, fluctuation of the earth tides, and irradiation from the sun (Lichtenberger 2005). Therefore, the recorded EMR signals are clear with minor disturbance and very low noisy level.

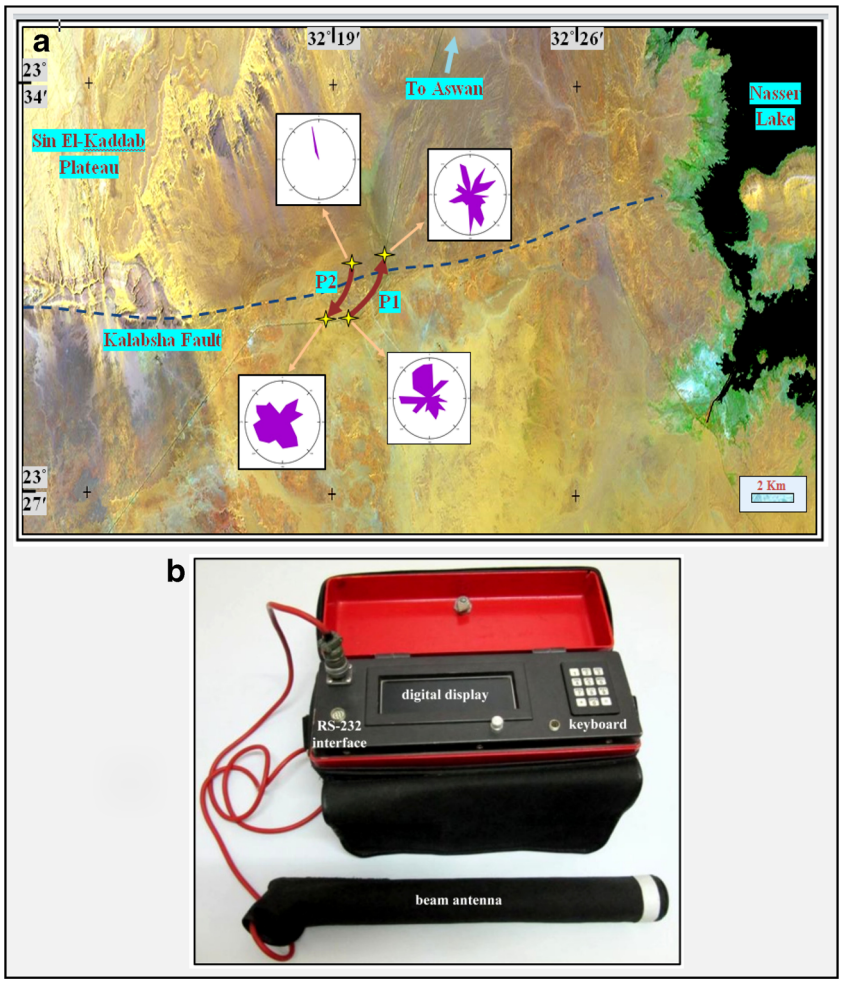


**Fig. 6** **a** Linear EMR profiles measured crossing the KFZ, **b** the Cerescope device

The two measured linear EMR profiles in KFZ are interpreted based on previous publications and studies as we have no standard or guided EMR profiles, yet. On the EMR intensity curves of each profile, the higher intensities are marked peaks. Each peak can be individually interpreted to define the nature of a fault or a fracture generating the signal. Figure 7 shows a possible interpretation for the different EMR peaks identified from the EMR profiles measured across the KFZ. In the same context, the inclined gray lines suggest steeply dipping faults having

**Table 1** Data sheet of the Cerescope measurements

| Object-Kalabsha___, Profile–2_____, 12.02.2015 11:15:57 | | | | | | | |
|---|---|---|---|---|---|---|---|
| Picket | Parameter A | Parameter B | Parameter C | Parameter D | Parameter E | Azimuth | Time |
| 1 | 16 | 0 | 0 | 0 | 0 | 0 | 12/02/2015 11:15 |
| 2 | 18 | 4 | 81 | 309 | 22 | 0 | 12/02/2015 11:15 |
| 3 | 36 | 4 | 51 | 171 | 22 | 0 | 12/02/2015 11:15 |
| 4 | 80 | 26 | 47 | 852 | 22 | 0 | 12/02/2015 11:15 |
| 5 | 86 | 28 | 94 | 373 | 22 | 0 | 12/02/2015 11:15 |

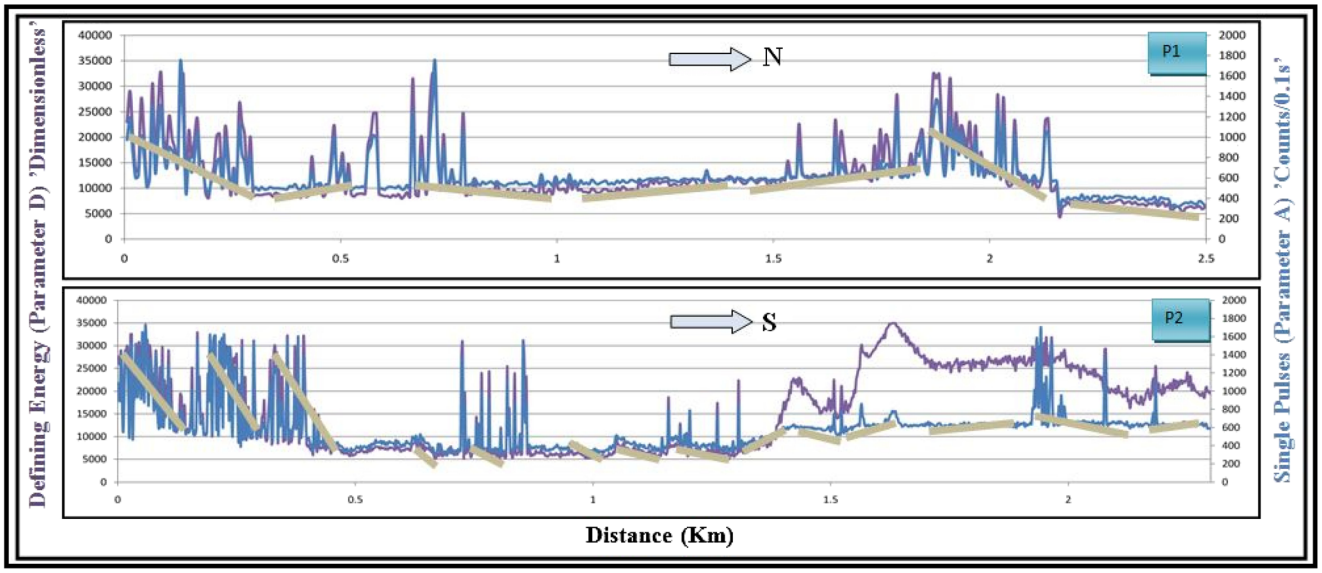


**Fig. 7** A possible interpretation for the different EMR peaks identified from the EMR profiles measured across the KFZ

the same degree of inclination of the line under consideration. Based on the EMR data and according to the structural setting of the mapped faults along the KFZ, a set of active fractures trending ENE-WSW and has steeply-dipping surfaces is identified. The ongoing activity along these fractures is proposed to reactivate the upper crustal levels and most probably controls the seismic cycle underneath the Kalabsha Fault Zone, due to coupling with the lower crustal levels.

Four horizontal EMR measurements are taken with reference to the two linear EMR profiles, recorded at the start and end of each profile (see Fig. 6a). Performing such horizontal measurements using the Cerescope aims at the identification of the direction of the maximum horizontal stress ($\sigma_H$). Analysis and interpretation of the polar diagrams of the horizontal EMR data indicate that the direction of maximum horizontal stress is dominantly ENE (065–085). A secondary direction of a horizontal stress oriented NW to NNW (125–160)

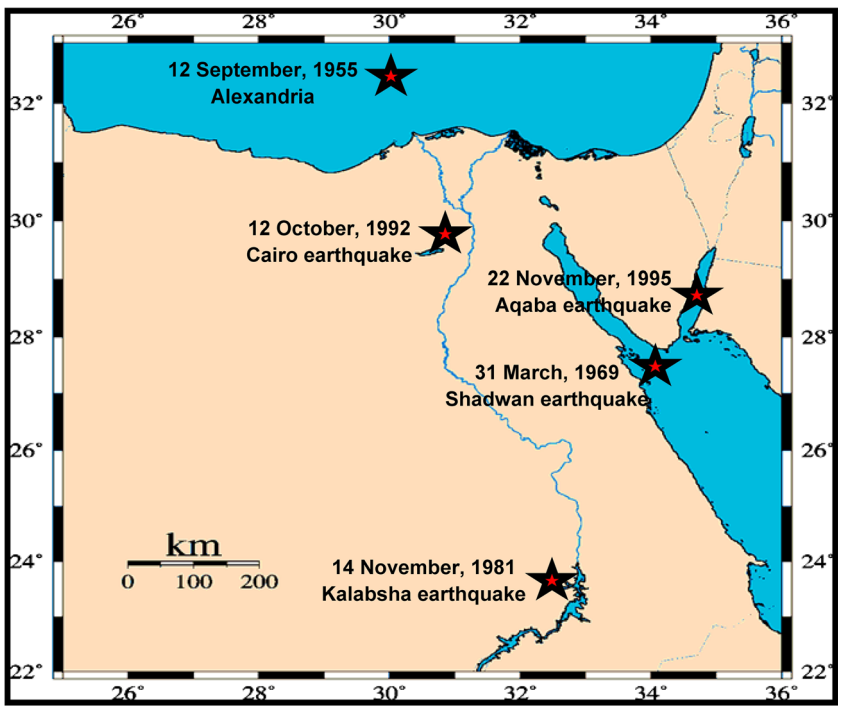


**Fig. 8** Historical earthquakes hitting Egypt and cause remarkable damage; realize the November 1981 event that caused a considerable damage in Aswan region, at KFZ

can also be estimated. These results refer to a current activity along the investigated part of the KFZ, which extends to the western margin of the Nasser Lake that lies directly to the south of Aswan High Dam.

## Seismicity of the Kalabsha Fault Zone

### Data collection and analysis

The present study is based mainly on the available seismological records obtained from the National Research Institute of Astronomy and Geophysics (NRIAG). Seismological data of the study area are collected from Egyptian National Seismological Network (ENSN) catalog for the period from January 1997 to December 2016. Earthquakes having the magnitudes of ML ≥ 3.2 are selected. The earthquake location is one of the most important parameters in applied seismology. The routine computation of locations may be affected by at least two sources of error: the unsuitable distribution of the recording stations and the presence of significant lateral variation in the earth that is not included in the routinely used one-dimensional (1D) velocity models. Both problems can be fixed by studying the detection capability of the network stations. Waveform data were analyzed using Atlas package software, which include a HYPOINVERSE program (Klein 1978) used to locate earthquakes with high proficiency. Since earthquake relocation is vital for many applications, including hazard forecasting and assessment, seismic tomography, stress field, and source mechanism studies, the selected earthquakes were stored after converting earthquake data from X–Y format to SEED in order to unify the data type read by the HYPOINVERS. Then, the crustal velocity models (i.e., crustal model of Aswan) were introduced to the program to get files containing earthquake location solution; hypocenter parameters (Lat., Long. and Depth), origin time, root mean squared residual RMS, vertical and depth error, local and duration magnitude, stations used in P and S picking, station distances from epicenter and calculated travel times to every station.

### Seismicity distribution

Spatial distribution of earthquake epicenters is very important, since the larger events take place along active faults or plate boundaries. Therefore, the epicenter distribution can be used to characterize these faults, plate boundaries, and define the direction of their motion. The seismicity pattern would be reliable if a large accurate, homogeneous, and complete data

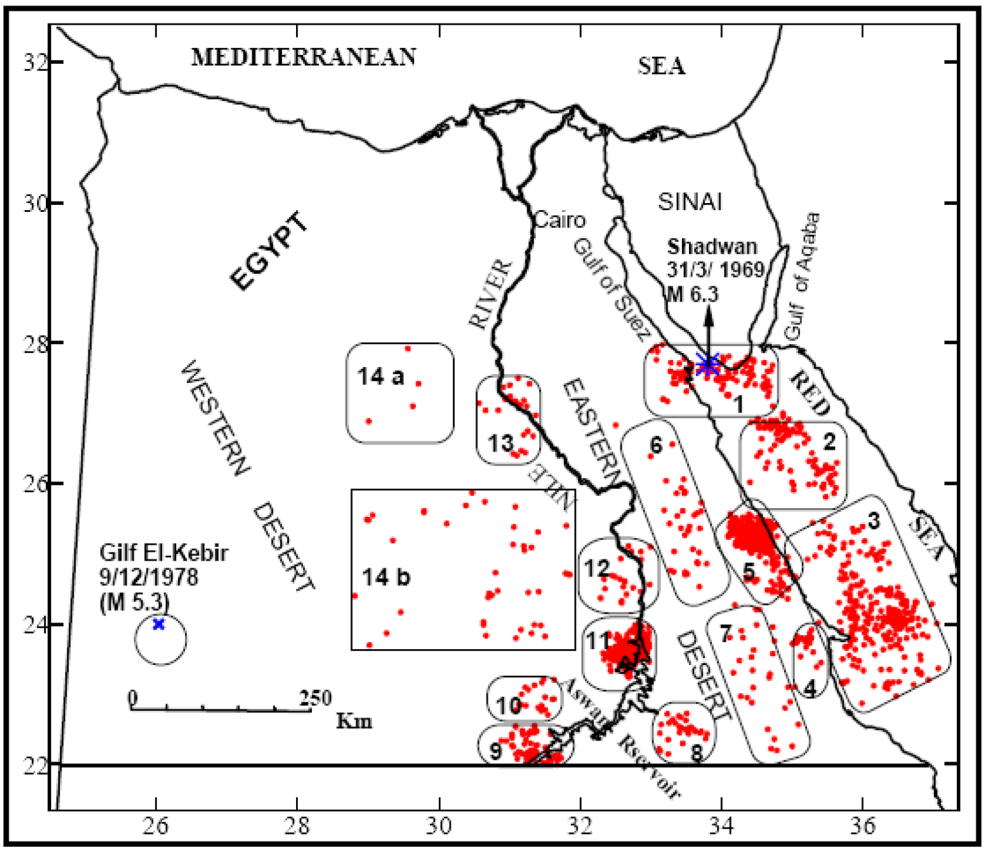


**Fig. 9** The seismic zones proposed by Haggag et al. (2008) according to seismicity level and spatial distribution of events in southern Egypt during the period from 1981 to 2006

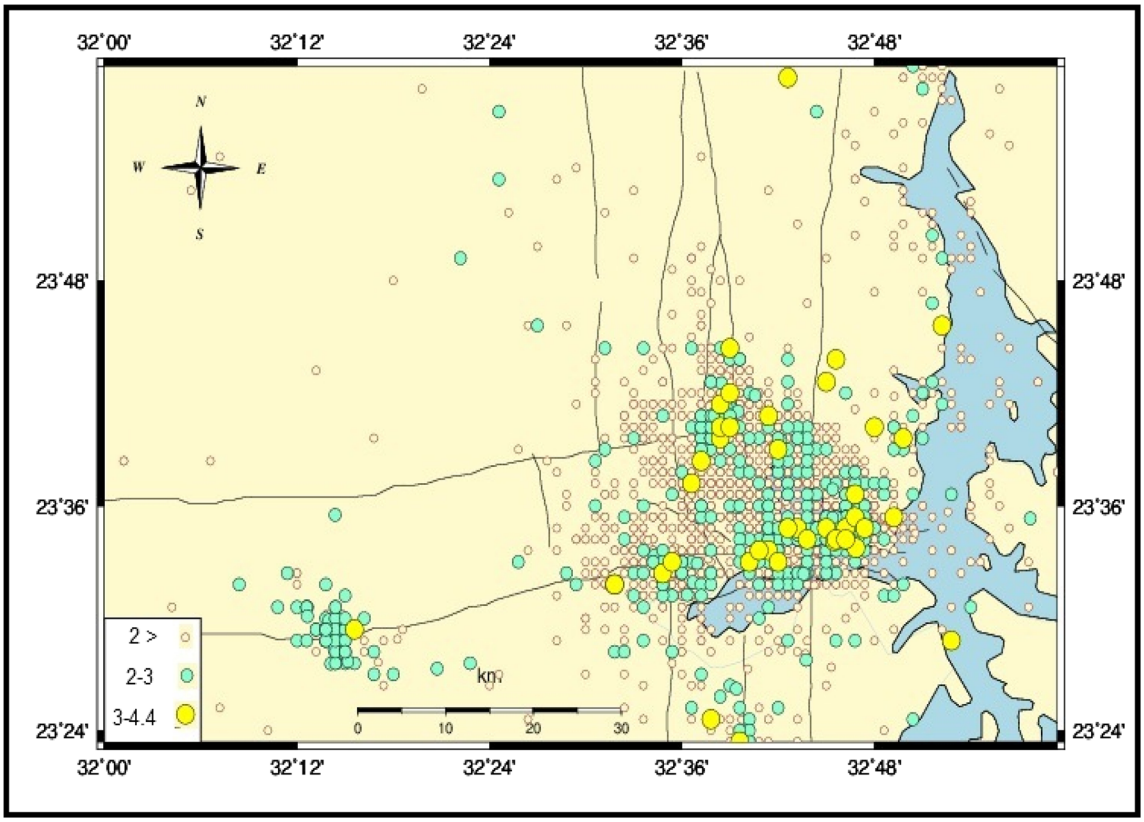


**Fig. 10** The geospatial distribution of the seismic activity in and around Nasser Lake from 1997 to 2016

set is used. So, the information of both historical and instrumentally recorded earthquakes is very important. Historical earthquake data, however, are used to assess the recent events and are very useful in forecasting seismic risk and mitigation of damage and human losses from future earthquakes, as it can give valuable information on the recurrence interval of each region (Ambraseys 1971; Badawy 1995, 1996, 1998). Egypt is considered as one of the few regions in the world where evidence of historical earthquake activity have been documented since 2200 B.C. Therefore, it is important to take into consideration catalogs of Maamoun et al. (1984) and Ambraseys et al. (1994) in which historical earthquakes are re-evaluated from all available original sources. The historical events that affected the study area are shown in Fig. 8.

Not long ago, the southern Egypt was known as aseismic zone except for few historical events that were documented in the annals of ancient Egyptian history and on some temples. Information about the instrumental earthquakes that occurred in southern Egypt before the Aswan 1981 earthquake were considered as historical earthquakes. The seismic activity in southern Egypt during the period 1981–2006 can be grouped according to the seismicity level and the spatial distribution into 14 seismic zones (Haggag et al. 2008) (Fig. 9). The higher distribution of the activity from the Red Sea coast towards the Nile River and Aswan region to the west, as well as the concentration of seismic activity in different seismic zones in E-W direction, were recognized. In addition, Haggag et al. (2008) studied the seismic activity in Aswan region and recognized 8 distinct sub-seismic zones, based on spatial distribution and the level of the seismicity: West High Dam, Northern old-stream channel, Southern old stream channel, Gebel Marawa, East Gebel Marawa, East-East Gebel Marawa, Khor El-Ramla, and Abou Dirwa. Woodward-Clyde Consultants (1985) concluded that the reservoir of Aswan itself does not produce earthquakes, but it can trigger the release of preexisting stress stored in the Earth's crust along few E-W and N-S faults crossing the area. Both water load and pore-fluid strain results have played a major role in triggering the shallower activity, while the pore-fluid pressure is the main factor triggering deeper activity (Woodward-Clyde Consultants 1985; Abu Elenean 2007).

In the study area, the spatial distribution of instrumental events (Fig. 10) for the period from 1997 to 2016 shows that many of the seismic events are clustered in definite zones along N–S and E–W fault trends. Few shocks are scattered far from the identified faults, probably related to some location errors. Along the KFZ, the seismicity is highly concentrated and its extension towards east is harmonic with the surface trace of the Kalabsha fault as the fault tip is directed toward the east, where concealed under the Lake Nasser and probably

define the most active seismic location along such zone. A cluster of seismicity along the faults trending N–S is also observed at the southern ends of both Khur El-Ramla and Kurkur faults. Low activity is relatively demonstrated in the N-S direction along Abou Dirwa fault and at the intersection of Gebel El-Barqa and Seiyal faults. It is clearly shown that most of the seismic activity is concentrated close to the intersection between the E-W and N-S trending faults and at their fault-tips. Figure 11a, b shows the E-W and N-S vertical cross sections along the hypocentral distribution of Kalabsha area.

## Focal mechanism solutions

### Methodology

The main aims of this section are to collect the previous fault-plane solutions of all earthquakes with local magnitude ML ≥ 3.2 recorded within the study area during the period from 1981 to 2016 and to construct new fault-plane solutions for some recent events based on the first motion polarities. The fault-plane solutions of the earthquakes in this area were studied by many authors (e.g., Abu Elenean. 1997; Badawy 2001; Hussein et al. 2013; Hosny et al. 2014; Abdelazim et al. 2016). In order to achieve the focal mechanism solution of earthquakes in Aswan region as a whole and in the Kalabsha area in specific, 10 earthquakes with magnitude ML ≥ 3.4 are selected. Such events have occurred in and around Nasser Lake during the time period from 2007 to 2016. The data of these earthquakes were extracted from the database of the Egyptian National Seismological Network (ENSN) as a digital waveform data (Table 2). These data are selected for making a reasonable focal mechanism solution along the KFZ in Aswan region. All the chosen events are relocated using the HYPOINVERSE program (Klein 1978) and the velocity model of the Aswan region to get highly accurate locations. The first motion polarities of P-wave picked from the digital waveform data are used in constructing the solutions. P-wave first motion is the simplest method to determine these solutions. The polarity of the onset P-wave arrival varies between seismic stations at different directions from an earthquake. The polarity of the first P-wave onset may be up (+) or down (−) according to the slip between the two fault blocks. If the fault block move toward the station, the polarity is called compression (+ up) in this station, and if it moves away from the station, the polarity is called dilatation (− down). By using the polarity of the first P-wave onset, the focal mechanisms of the events have been achieved using the software package developed by Suetsugu (1998).

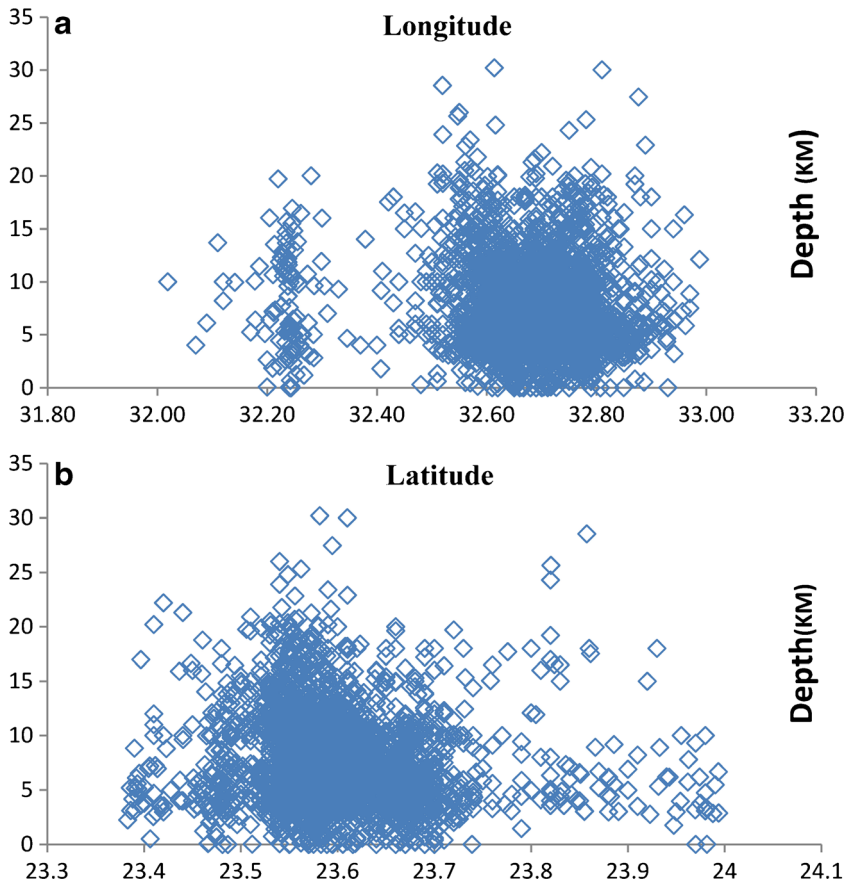


**Fig. 11** **a** The E-W and N-S and **b** depth profiles across the hypocentral distribution along the KFZ for the events from 1997 to 2016

**Table 2** The seismic parameters and focal mechanism solutions of the10 selected events along the KFZ

| No | Date Y-M-D | Time H:M:S | Location | | Depth (km) | ML | P-axis AZ-PL | T-axis AZ-PL | Nodal plane 1 | | | Nodal plane 2 | | |
|---|---|---|---|---|---|---|---|---|---|---|---|---|---|---|
| | | | Lat. | Long. | | | | | Strike | Dip | Rake | Strike | Dip | Rake |
| 1 | 2007-04-12 | 14:19:22 | 23.59 | 32.71 | 13.8 | 3.8 | 306–24 | 036–01 | 84 | 73 | − 163 | 349 | 74 | − 18 |
| 2 | 2008-10-23 | 21:28:29.09 | 23.59 | 32.72 | 4.28 | 3.42 | 295–11 | 025–01 | 70 | 82 | − 173 | 339 | 83 | − 8 |
| 3 | 2009-02-10 | 23:43:3.96 | 23.59 | 32.76 | 25.5 | 3.9 | 307–13 | 039–08 | 84 | 75 | − 176 | 353 | 86 | − 15 |
| 4 | 2009-07-29 | 00:12:50.05 | 23.58 | 32.75 | 6.33 | 3.38 | 111–25 | 014–14 | 245 | 83 | − 152 | 151 | 62 | − 8 |
| 5 | 2010-03-13 | 02:22:16 | 23.57 | 32.78 | 7.68 | 3.87 | 122–05 | 212–01 | 257 | 86 | − 178 | 167 | 88 | − 4 |
| 6 | 2011-12-26 | 17:01:26 | 23.55 | 32.59 | 10.1 | 4.1 | 306–12 | 037–05 | 351 | 85 | − 13 | 82 | 78 | − 175 |
| 7 | 2013-10-27 | 13:21:42.97 | 23.57 | 32.72 | 3.56 | 3.85 | 121–12 | 213–07 | 167 | 86 | − 13 | 258 | 77 | − 176 |
| 8 | 2015-11-21 | 15:53:22.04 | 23.57 | 32.78 | 9.02 | 3.35 | 303–45 | 035–02 | 89 | 58 | − 146 | 339 | 61 | − 37 |
| 9 | 2016-09-19 | 21:50:54.08 | 23.57 | 32.71 | 6.3 | 3.63 | 298–14 | 030–07 | 75 | 75 | − 175 | 343 | 85 | − 15 |
| 10 | 2016-09-21 | 12:35:47.14 | 23.57 | 32.71 | 3.91 | 3.40 | 123–12 | 033–00 | 259 | 82 | − 172 | 168 | 82 | − 8 |

## Data analysis and interpretation

In the present study, the focal mechanism solutions of 28 earthquakes with magnitude ML ≥ 3.2 are compiled from previous studies during the period from 1981 to 2016 (Abu Elenean 1997; Badawy 2001; Abdelazim et al. 2016). The majority of these solutions (Fig. 12) show that the two nodal planes are striking ENE-WSW to E-W and NNW-SSE to N-S. Most of the fault plane solutions indicate right-lateral strike-slip movement with a minor vertical component. However, the focal mechanism solutions of the 10 recent earthquakes have been resolved (Table 2) and graphically represented (Fig. 13a, b).

Occasionally, the mechanism of a single earthquake is unconstrained due to insufficient seismic data. Therefore, composite fault plane solutions are considered to lump together all events in a localized area at nearly the same depth to infer the most probable mechanism for the source. This can improve the data recovery by combining all the first motions into one data set, where the best solution could be obtained. Eight earthquakes were collected from the ENSN catalog and lumped together in one composite solution (Fig. 13c). The hypocenter parameters of these events and their composite fault plane solutions are shown in Table 3. The constructed mechanisms by applying such method indicate a well-considered seismic fault strikes N77°E with dip and rake

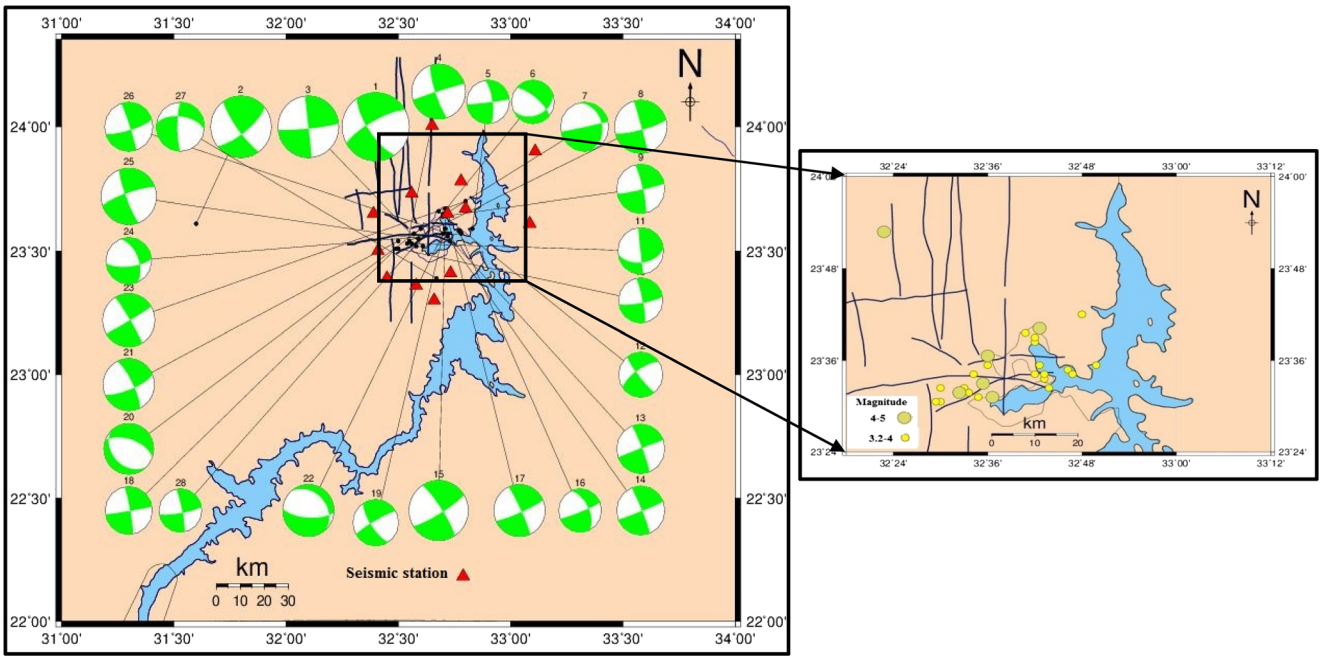


**Fig. 12** The focal mechanisms of earthquakes with magnitude ML ≥ 3.2 (1981–2016) distributed at Aswan area after CMT Harvard and ENSN, Badawy (2001), Abu Elenean (1997), and Abdelazim et al. (2016)

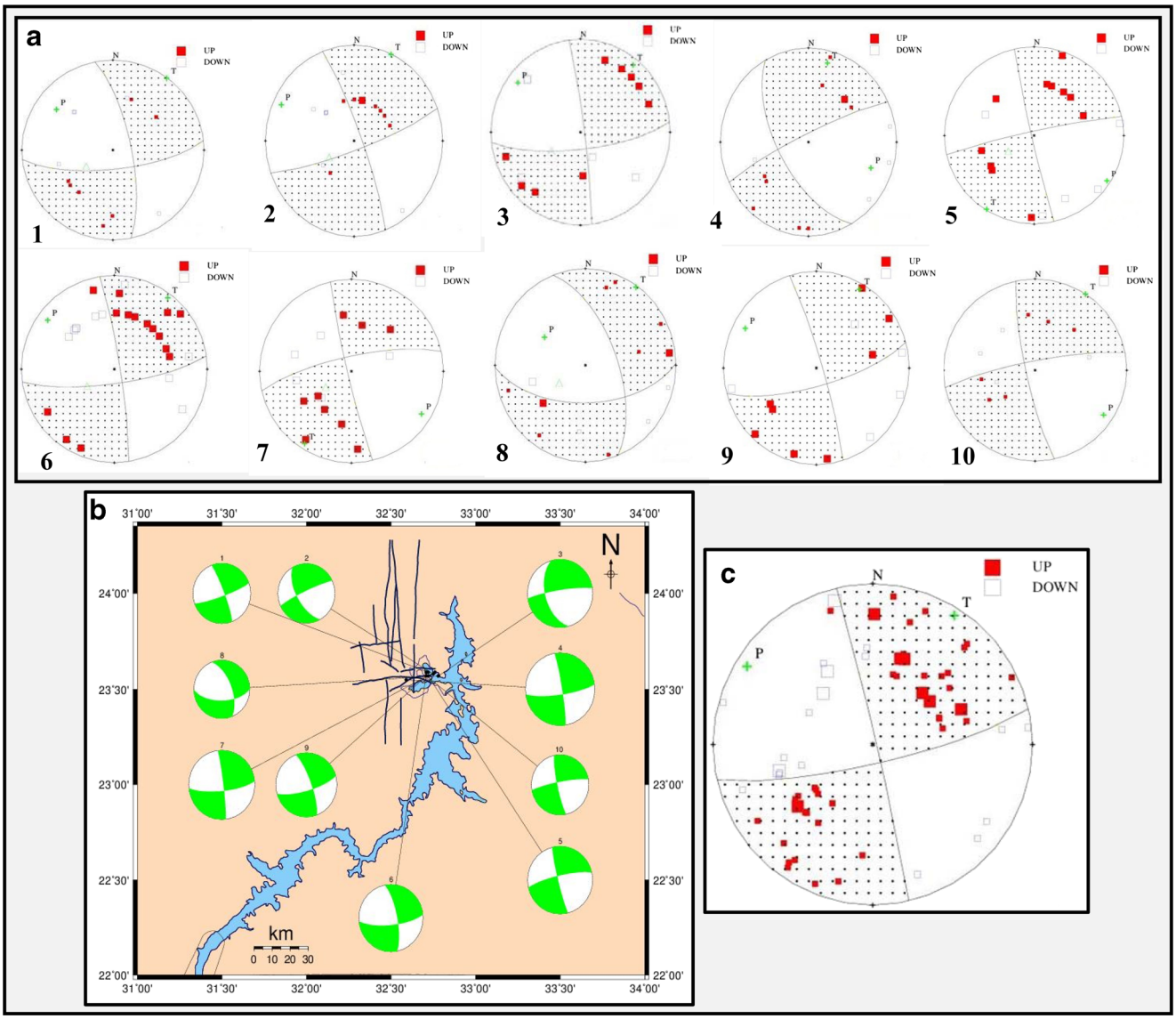


**Fig. 13** **a** Fault plane solutions, **b** focal mechanisms of 10 recent earthquakes, and **c** composite focal mechanism solution of selected 8 events located within the KFZ. Nearly all solutions show nodal planes trending ENE-WSW to E-W and NNW-SSE to N-S

angles of 88°NNW and − 178°, respectively. The parameters of the auxiliary plane are N13W, 88° WSW, and − 10°, respectively. The P and T axes have azimuth and plunges of 302°, 8° and 032°, 6°, respectively. Also, this mechanism demonstrates the same sense of movement for each event as a major dextral strike-slip with minor normal dip-slip component.

Concisely, the main results of the two types of earthquake focal mechanisms (first motion polarity and composite fault plane solutions) demonstrate two nodal planes; one striking ENE-WSW to E-W and showing right-lateral strike-slip movement, while the other strikes NNW-SSE to N-S with left-lateral movement. The focal mechanisms of the mainshocks are in agreement with the surface traces of the Kalabsha Fault. The tensional stresses are prevailing in NE-SW direction, whereas the compressive stresses are prevailing in NW-SE direction. Generally, the main faulting mechanism in Aswan region is wrenching movement associated with minor vertical dip-slip component as a consequence of the present-day prevailing trasnstensional tectonic regime.

## Summary and conclusions

The present work is an integrated study that aims at unraveling the structural setting and seismotectonic activity associated with the KFZ. The study of major tectonic trends using field-structural investigation, identification of maximum

**Table 3** The hypocenter and the composite fault-plane solution parameters of the eight elective events

| No | Date Y-M-D | Time H:M:S | Location | | Depth (km) | ML |
|---|---|---|---|---|---|---|
| | | | Lat. | Long. | | |
| 1 | 1982–07-13 | 21:44:3.89 | 23.56 | 32.57 | 15.86 | 3.3 |
| 2 | 1982–08-20 | 18:21:3.36 | 23.57 | 32.55 | 16.47 | 2.4 |
| 3 | 1983–01-05 | 14:58:0.16 | 23.56 | 32.55 | 17.47 | 3.4 |
| 4 | 1983–01-11 | 08:12:57.05 | 23.55 | 32.57 | 17.30 | 3.0 |
| 5 | 1984–02-22 | 06:20:1.48 | 23.55 | 32.58 | 16.35 | 3.3 |
| 6 | 1984–02-24 | 03:21:1.78 | 23.55 | 32.57 | 15.35 | 3.3 |
| 7 | 1987–09-24 | 10:16:24.94 | 23.54 | 32.57 | 17.37 | 2.7 |
| 8 | 1987–10-07 | 04:35:31.56 | 23.55 | 32.57 | 17.70 | 3.1 |

| P-axis AZ-PL | T-axis AZ-PL | Nodal plane 1 Strike Dip Rake | Nodal plane 2 Strike Dip Rake |
|---|---|---|---|
| 302–08 | 32–06 | 77 88 -178 | 347 88 -10 |

horizontal stress orientations using EMR technique and analysis of the seismicity and fault-plane mechanisms are good tools for such integrated work. Based on structural-field observations, the first-order interpretation of the KFZ is that it is not a simple transcurrent wrench fault with dextral sense of movement but, however, it is a major dextral transtensional shear zone deforming the southern Egypt and controls the seismotectonic setting of the area to the west of Nasser Lake. Transtensional regime can be ascribed partially here in the term of an extensional tectonics that accommodated by the formation of NW-trending normal faults during the opening of the Red Sea. The transtension possesses a post-Lower Eocene age and cuts through nearly all rock units of the Upper Cretaceous Nubia Sandstone and the overlying Paleocene-Lower Eocene Krukur, Garra and Dungul formations, as well as the Quaternary sedimentary cover. Topographic expression of KFZ as well as the seismicity distribution suggests that the fault changes its geometry from west to east, as it is evidently realized in Sinn El-Kaddab Scarp to the west and at Gebel Marawa to the east.

Seismological investigations of the well-located epicenters recorded by ENSN from January 1997 to December 2016 have shown that the majority of the local earthquakes are largely concentrated along the Kalabsha Fault and its augmentation towards east in harmony with the surface trace of this fault as one of the evidence that advocate faulting activity. The linear alignment of the aftershocks distribution helps to define the most active plane of the Kalabsha Fault. In addition, faults rarely occurred individually but form sets or networks at faults intersection, where the loci of intensified seismicity and stress localization. Earthquake focal mechanisms employed in this study for understanding the nature of earthquakes, where the data extracted from the focal mechanism solutions (FMS) are of much importance to determine the present day active stress pattern that in turn contribute to the tectonic setting causes the earthquake activity. Focal mechanisms of 28 earthquakes with magnitude ≥ 3.2 are compiled from previous publications covering the period from 1981 to 2016 in contrast with the source mechanisms constructed in this study for 10 recent earthquakes. Focal mechanism solutions of such 10 earthquakes, recorded by ENSN from the period of 2007 to 2016 with magnitude ≥ 3.4, have been constructed based on the first motion polarities of P-wave. Composite fault-plane solutions are considered to lump together 8 selected events in a localized area at close to the equal depth to infer the most probable source area mechanism. In approximation, all source mechanisms show the same results; the displacement along the Kalabsha Fault Zone is strike-slip with minor vertical dip-slip component. The focal mechanism solutions indicate two orthogonal nodal planes striking E to ENE with subordinate right-lateral strike-slip component and N to NNW with opposite left-lateral motion. Meanwhile, the directions of tectonic extension (T) and compression (P) are NNE-SSW and NNW-SSE, respectively.

Regarding the reactivation of KFZ, the principal area is Gebel Marawa Zone, which is the epicenter of the mainshock of the November, 1981 earthquake that occurred along the fault zone. However, some of the recent earthquakes are located along the ENE-WSW oriented KFZ and indicate dextral focal mechanisms, suggesting present-day reactivation of the fault zone. Meanwhile, the anticlinal structure at Gebel Marawa invokes some of the Kinematic history of such zone, where a faulting event with a vigorous movement passing into periods of crushing, grinding, and pulverization. Therein, the fault breccia and fault gouge represent the tectonits produced during such event. Furthermore, recording of slickenside lineations on some fault surfaces deforms the most recent rock units that indicate recent reactivation of the fault zone. Offsetted Quaternary deposits unconformably overlying the Dungul Formation (including conglomerate sheets, tufa and playa deposits, sand dunes, and reworking fresh-water limestone), which are distributed near the scarp face between Gebel Kalabsha and Gebel El-Digm, indicate a recurrent motion during the Quaternary. The presence of ground cracks (sand channels) that developed near the surface trace of Kalabsha Fault between Gebel Kalabsha and Gebel Marawa and filled with fine wind-blown sand indicating ongoing activity on the Kalabsha Fault Zone. Such well-developed surface rupturing is relatively narrow zones of few tens of meters to as 200 m length and as wide as approximately 0.5 m (Woodward-Clyde Consultants 1985). Also, the EMR data suggest a new phase of activity along the KFZ, where the direction of the main horizontal stress σ1 is perturbed between ENE and NNW directions. These results point to an active fault system oriented ENE-WSW and NNW-SSE, affecting such area and running through the KFZ.

**Acknowledgments** Authors would like to thank Prof. Awad Hassoup, Head of Seismology Department in the National Research Institute of Astronomy and Geophysics (NRIAG), for great help and offering facilities for data to achieve this work. We are also grateful to Prof. Hesham Hussein, Head of National Data Center (NRIAG), for fruitful recommendations, and to Dr. Saud Abdallah in Seismology Department (NRIAG) for helpful cooperation.

## References

Abdeen MM, Abdelsalam MG, Nielsen KC, Yehia MA, Cherif OH (2000) Active dextral wrenching in southern Egypt. In 38th Annual Meeting of the Geological Society of Egypt, Cairo, November

Abdelazim M, Samir A, El-Nader IA, Badawy A, Hussein H (2016) Seismicity and focal mechanisms of earthquakes in Egypt from 2004 to 2011. NRIAG J Astron Geophys 5(2):393–402

Abu Elenean KM (1997) A study on the seismotectonics of Egypt in relation to the Mediterranean and red seas tectonics. Ph. D. Thesis, Faculty of Science, Ain Shams University, Cairo, Egypt

Abu Elenean KM (2007) Focal mechanisms of small and moderate size earthquakes recorded by the Egyptian National Seismic Network (ENSN), Egypt. NRIAG J Geophys 6(1):119–153

Ambraseys NN (1971) Value of historical records of earthquakes. Nature 232:375–379

Ambraseys NN, Melville CP, Adams RD (1994) The seismicity of Egypt, Arabia and the Red Sea. A historical Review, Cambridge

Attia MI (1955) Topography, geology and iron-ore deposits of the district east of Aswan: Cairo. Egypt. Geol. Survey Dept, Abbassia, Egypt

Awad M, Mizoue M (1995) Earthquake activity in the Aswan region, Egypt. Pure Appl Geophys 145(1):69–86

Badawy A (1995) Source parameters and tectonic implications of recent Sinai (Egypt) earthquakes. Acta Geod Geoph Hung 30:349–361

Badawy A (1996) Seismicity and kinematic evolution of the Sinai plate. Ph.D. thesis, L. EotvosUniv ., Budapest

Badawy A (1998) Historical seismicity of Egypt. Acta Geod Geoph Hung 34(1–2):119–135

Badawy A (2001) Status of the crustal stress in Egypt as inferred from earthquake focal mechanisms and borehole breakouts. Tectonophysics 343(1):49–61

Bahat D, Rabinovitch A, Frid V (2005) Tensile fracturing in rocks-tectonofractographic and electromagnetic radiation methods, vol 16. Springer, 570 pp

El Etr HA, Yehia MA, Dowidar H (1982) Fault pattern in the south Western Desert of Egypt. Ain Shams Univ Sci Res Ser 2:123–152

El-Hady SM, Khalil AE, Hosny A (2004) 1-D velocity structure in northern of Aswan Lake, Egypt deduced from travel time data. J Appl Geophys 3(1):55–62

El-Shazly MS (1954) Rocks of Aswan area. Governmental Press

Fat-Helbary R, Tealeb A (2000) A study of seismicity and earthquake loading at the proposed Kalabsha dam site, Aswan, Egypt. Bulletin of NRIAG B, 39-61

Greiling RO, Obermeyer H (2010) Natural electromagnetic radiation (EMR) and its application in structural geology and neotectonics. J Geol Soc India 75(1):278–288

Guiraud R, Bosworth W (1997) Senonian basin inversion and rejuvenation of rifting in Africa and Arabia: synthesis and implications to plate scale tectonics. Tectonophysics 282:39–82

Guiraud RO, Bosworth W (1999) Phanerozoic geodynamic evolution of northeastern Africa and the northwestern Arabian platform. Tectonophysics 315(1):73–104

Guiraud RO, Issawi B, Bosworth W (2001) Phanerozoic history of Egypt and surrounding areas. Peri-Tethys Memoir 6:469–509

Hagag W, Obermeyer H (2017) Active structures in central Upper Rhine Graben, SW Germany: New data from Landau area using Electromagnetic Radiation (EMR) Technique and Cerescope. J. Geol. Geophys 6(5) in press

Haggag HM, Gaber HH, Sayed AD, Ezzat ME (2008) A review of the recent seismic activity in the southern part of Egypt (upper Egypt). Acta Geodyn Geomater 5(1):19–29

Hamimi Z, Hagag W (2017) A new tectonic model for Abu-Dabbab seismogenic zone (Eastern Desert, Egypt): evidence from field-structural, EMR and seismic data. Arab J Geosci 10(1):11

Hassib GH (1997) A study on the earthquake mechanics around the high dam Lake, Aswan, Egypt. Ph. D. Thesis, Faculty of Science, South Valley University, Sohag, Egypt

Hogan JP, Tewksbury BJ, Mehrtens C, Ellis T (2013) The Desert Eyes project Part II: Structures along East-West and North-South faults of the Western Desert, Egypt. In Geological Society of America Abstracts with Programs 45(7), p. 160

Hosny A, Ali SM, Abed A (2014) Study of the 26 December 2011 Aswan earthquake, Aswan area, south of Egypt. Arab J Geosci 7(11):4553–4562

Hussein HM, Elenean KA, Marzouk IA, Korrat IM, El-Nader IA, Ghazala H, El Gabry MN (2013) Present-day tectonic stress regime in Egypt and surrounding area based on inversion of earthquake focal mechanisms. J Afr Earth Sci 81:1–15

Issawi B (1968) The geology of Kurkur-Dungle area. Geol Surv Egypt, paper 46, p. 102

Issawi B (1969) The geology of KurkurDungul area.US Government Printing Office

Issawi B (1973) Nubia sandstone: type section. AAPG Bull 57(4):741–745

Issawi B (1978) Geology of Nubia west area, Western Desert, Egypt. Ann Geol Surv Egypt 8:237–253

Issawi B (1982) Geology of the Southwestern Desert of Egypt. Annal Geol Surv of Egypt

Issawi B (1987) Geology of the Aswan Desert. Annals Geol. Survey of Egypt

Issawi B, Jux U (1982) Contributions to the stratigraphy of the Paleozoic rocks in Egypt. Geol. Surv. of Egypt

Issawi B, Osman RA (1993) Tectonic-sedimentary synthesis of Paleozoic-cretaceous clastics, SW Aswan, Egypt. J Sed Egypt 1: 11–22

Kebeasy RM, Tealab A (1997) Earthquake activity and subsurface structures of south valley project. Internal report. Natl Res Inst Astron Geophys 14:1–87

Kebeasy RM, Maamoun M, Ibrahim EM (1981) Lake Aswan induced earthquake. Bull Internal Inst Seismol Earthq Eng 19:155–160

Kebeasy RM, Maamoun M, Ibrahim E, Megahed A, Simpson DW, Leith WS (1987) Earthquake studies at Aswan reservoir. J Geodyn 7(3–4): 173–193

Khalil AE, El-Hady SM, Hosny A (2004) Three-dimensional velocity structure of VP and VP/VS around Aswan area, Egypt.J Appl. Geophys 3(1):303–314

Klein FW (1978) Hypocenter locations program HYPOINVERSE. US Department of the Interior, Geological Survey

Lauterbach M (2005) Beurteilung der Eignung der NPEMFE-Methode (Natural Pulsed Electromagnetic Field of Earth) mit dem "Cereskop" in Rutschungen und in Lockerund Festgesteinen mit Spannungsänderungen im Mittel- und Hochgebirge Ph.D. Thesis University of Mainz , 243 pp.

Lichtenberger M (2005) Regional stress field as determined from electromagnetic radiation in a tunnel. J Struct Geol 27:2150–2158

Lichtenberger M (2006a) Bestimmen von Spannungen in der Lithosphäre aus geogener elektromagnetischer Strahlung. Ph.D. Thesis University of Heidelberg (140 pp)

Lichtenberger M (2006b) Underground measurements of electromagnetic radiation related to stress-induced fractures in the Odenwald Mountains (Germany). Pure Appl Geophys 163:1661–1677

Maamoun M, Megahed A, Allam A (1984) Seismicity of Egypt. Bull Helwan Inst Astron Geophys 4(B):109–132

Mahmoud SM (1994) Geodetic and seismotectonic deformation near Aswan reservoir, Egypt. Bulletin of CRCM 41, Praha, Czech Republic, pp. 5–30

Mallik J, Mathew G, Angerer T, Greiling RO (2008) Determination of directions of horizontal principal stress and identification of active faults in Kachchh (India) by electromagnetic radiation (EMR). J Geodyn 45:234–245

Mekkawi M, Abdel-Monem SM, Rayan A, Mahmoud S, Saleh A, Moustafa S (2008) Subsurface Tectonic Structure and Crustal Deformation at Kalabsh fault, Aswan, Egypt from Magnetic, GPS and Seismic data. NRIAG J Geophys, special issue, pp 681–700

Meshref WM (1990) Tectonic framework of Egypt. In: Said R (ed) Geology of Egypt. A.A. Balkema Publisher, Netherland, pp 113–153

Obermeyer H (2001) Handbuch zur Anwendung der EMR-Methode mittels des Cereskops. Ceres GmbH, Staffort (32 pp)

Obermeyer H (2005) Measurement of natural pulsed electromagnetic radiation (EMR) with the Cerescope. Ceres GmbH, Staffort

Obermeyer H, Lauterbach M, Krauter E (2001) Monitoring landslides with natural electromagnetic pulse radiation. In: International Conference on Landslides, pp. 297–304

Reuther C, Moser E (2009) Orientation and nature of active crustal stresses determined by electromagnetic measurements in the Patagonian segment of the South America plate. Int J Earth Sci 98:585–599

Reuther C, Obermeyer H, Reicherter K, Reiss S, Kaiser A, Buchmann T, Adam J, Lohrmann J, Grasso M (2002) Neotectonic und active Krustenspannung in Südost- Sizilien und ihre Beziehungzurregionalen Tektonikim Zentralen Mittelmeer. Mitt Geol Palaontol Inst Univ Hamburg 86:1–24

Spinks SC, Parnell J, Bowden SA (2010) Reduction spots in the Mesoproterozoic age: implications for life in the early terrestrial record. Int J Astrobiol 9(4):209–216

Stern RJ, Abdelsalam MG (1996) The origin of the great bend of the Nile from SIR-C/X-SAR imagery. Science 274(5293):1696–1698

Suetsugu D (1998) Practice on source mechanism II SEE lecture note. Tsukuba, Japan, 104 pp

Taha YS (1997) Evaluation of the crustal structure setting of Aswan area. Ph.D. thesis, Faculty of Science, Cairo University, Egypt, 152 p

Tealeb A (1999) Proposed programs for monitoring crustal deformations at seismoactive area of Aswan, Egypt using geodetic techniques.Internal Report at NRIAG, 81p

Tewksbury B, Abdelsalam MG, Hogan JP, Jerris TJ, Pandey A (2009) Reconnaissance study of domes and basins in Tertiary sedimentary rocks in the Western Desert of Egypt using high resolution satellite imagery. In Geological Society of America Abstracts with Programs 41, No. 7, p. 458

Thurmond AK (2002) Understanding the structural control of the Nile through Batn El Hajar region, Northern Sudan using remote sensing imagery. M.Sc. thesis, Department of Geosciences, University of Texas at Dallas, pp. 348

Thurmond AK, Stern RJ, Abdelsalam MG (2000) Structural analysis of the cataract Nile in northern Sudan using Landsat TM and SIR-C/X-SAR Imagery.Abstract, international conference on the Western Desert, NARSS-EGSMA, p.12-13

Thurmond AK, Allison K, Stern RJ, Mohamed G, Abdelsalam MG, Kent D, Nielsen C, Abdeen MM, Hinz E (2004) The Nubian swell. J Afr Earth Sci 39:401–407

Woodward-Clyde Consultants (1985) Earthquake activity and stability evaluation for the Aswan high dam. Unpublished report, High Aswan and Dam Authority, Ministry of Irrigation, Egypt